The assessment of the ride quality of a truck-full trailer combination

Bor-Tsuen Wang and Po-I Hu

Department of Mechanical Engineering, National Pingtung University of Science and Technology, Pingtung, Taiwan 91207, Republic of China

E-mail: wangbt@mail.npust.edu.tw

Abstract: This paper presents an analytical model for the evaluation of the ride quality of A tractor and trailer moving on an irregular road surface. A nine degree-of-freedom tractor and trailer ride model is developed, and this is assumed to have a displacement input of a stationary ergodic Gaussian random road profile. The frequency response functions of the system are first derived so as to determine the power spectral density functions of the system response. A conventional tractor and trailer combination is then used to simulate the vehicle response, and thus the ride quality can be studied. The ride comfort of the driver's seat is evaluated in comparison to the ISO 2631. The suspension travel, road holding, dynamic tyre force and the acceleration distributions of the tractor and trailer that can affect the ride quality of parts and cargoes are also studied. The effects of the vehicle speed, laden and road roughness on ride quality are systematically evaluated.

Keywords: heavy vehicles, ride comfort, tractor and trailer, vehicle model.

Reference to this article should be made as follows: Bor-Tsuen Wang and Po-I Hu (1998) 'The assessment of the ride quality of a truck-full trailer combination,' *Heavy Vehicle Systems*, A Series of the *Int. J. of Vehicle Design*, Vol. 5, Nos 3/4, pp. 208–235.

1 Introduction

The needs of fast transportation frequently demand different kinds of tractors and trailers. The ride quality of such a vehicle is of great concern. The driver's comfort is known to greatly affect his fatigue and handling performance. The vibration amplitude of the cargo and the performance of the vehicle parts, such as the engine mounting, suspensions, tyres and the wheel axles, are factors that will also affect ride quality. The road condition has an important influence on ride quality; however, the road condition cannot be sufficiently controlled. The proper design of vehicle components is the only way to improve ride quality.

Ride quality is generally evaluated by measuring the ride comfort of the driver in comparison to comfort criteria. Various criteria have been developed to assess the ride comfort of the driver as well as the cargo. The ISO 2631 (ISO, 1978) provides a

vibration level for defining human tolerance to whole-body vibration. The averaged absorbed power (Lee and Prado, 1968; Stikeleather, 1978) associated with vertical and horizontal vibration transmitted to the driver can be a measure of ride quality at the driver's location. The comfort index (Ravalard and Coutellier, 1994) rated between 1 and 5, can be adopted to evaluate the ride comfort of passenger or cargo.

The development of the ride model is the primary task in studying the ride quality of a vehicle. A simple quarter car model is frequently used to assess ride quality (Raba, 1974; Dahlberg, 1979; Hac, 1985). The suspension and tyres can be modelled as a linear spring damper element for convenience and simplicity. The seat cushion can also be included in the dynamic model. To represent realistically the vehicle dynamics in more detail, either a half or full vehicle model can be developed based on the need for analysis objectives (Demic, 1992; ElMandry, 1987). The half vehicle model can usually provide the vertical and longitudinal responses, while the full model can additionally study the roll and lateral responses. The flexibility of vehicle body is also known to be critical to the response. The beaming effect of vehicle body can also be included in the ride model (Vaduri and Law, 1993; Magolis and Edeal, 1989)

Some nonlinear effects for suspensions and tyres can also be considered (Elmadary and Abduljabbar, 1990; Clark, 1981). Using the linearlization technique (Iwan and Yang, 1972; Atalik and Utku, 1976; ElMandany and Dokanish, 1980), the system response can usually be obtained. Depending on different types of road surface condition, such as a protruding surface, a periodically uneven road or a random road profile, different analysis procedures can be adopted (Dohi and Maruyama, 1990). The frequency domain analysis (Sun, 1987; Del Castillo *et al.*, 1990) is generally adopted for the random excitation, while the time domain analysis (Pintado and Benitez, 1990) can be used for specific types of road input.

This paper concerns the development of a half model of the truck and full trailer for the purpose of ride quality analysis. An irregular random road profile is taken as the road input; the frequency domain analysis is therefore adopted in this work. The ride quality parameters, including the ride comfort of the driver, accelerations at the different locations of the tractor and trailer, suspension travel, road holding and dynamic tyre force are all studied. The effects of vehicle speed, laden and road conditions on the ride quality are also considered. The developed analytical riding model can also be utilized for the optimum design of the system parameters.

2 Truck and full trailer riding model

The 9 DOF vehicle riding model is shown in Figure 1. z_1, z_2, z_3 and z_4 are the response coordinates of the unsprung masses m_1, m_2, m_3, m_4; z_5 and θ_1 are the vertical and pitch response coordinates of the tractor; θ_2 and θ_3 are the pitch responses of draw bar and trailer, respectively.

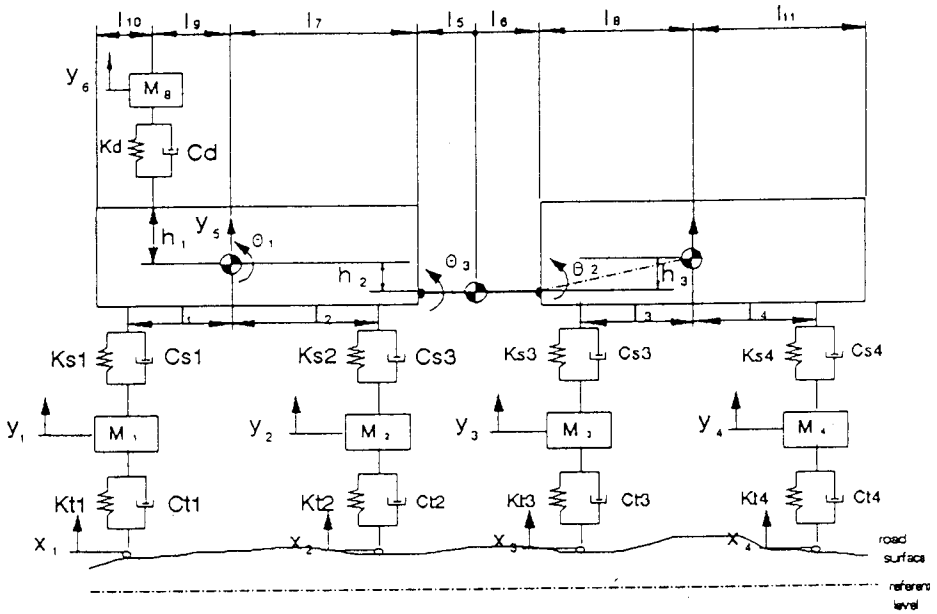

Figure 1 *9 DOF truck and full trailer riding model.*

The following assumptions are made:

1 The vehicle is moving at a constant forward speed over an uneven road.

2 The vehicle units (tractor, draw bar and trailer) are rigid.

3 The vehicle units are symmetric about the forward direction.

4 The tractor and trailer can translate in the vertical and pitch directions only.

5 The unsprung mass (wheel axle weight) is assumed to be connected between the suspension and the tyre.

6 Tyres are simulated as point contact models.

7 The tyre and suspension are assumed to be linear-spring-dampers.

The equations of motion of the full tractor trailer can be derived as follows:

$$[M]\{\ddot{y}\}+[C]\{\dot{y}\}+[K]\{y\}=[C]\{\dot{x}\}+[K]\{x\} \tag{1}$$

where

$$\{y\}^T=\{z_1 \quad z_2 \quad z_3 \quad z_4 \quad z_5 \quad z_8 \quad \theta_1 \quad \theta_2 \quad \theta_3\}$$

$$=\{y_1 \quad y_2 \quad y_3 \quad y_4 \quad y_5 \quad y_6 \quad y_7 \quad y_8 \quad y_9\} \tag{2}$$

$$\{x\}^T=\{x_1 \quad x_2 \quad x_3 \quad x_4\} \tag{3}$$

$\{y\}$, $\{\dot{y}\}$ and $\{\ddot{y}\}$ are the displacement, velocity and acceleration vectors of the output response coordinates respectively. $\{x\}$ and $\{\dot{x}\}$ are the displacement and velocity vectors of the input road profile respectively. $[M]$, $[C]$, $[K]$, $[C']$, $[K']$ are shown in Appendix A.

3 Road model

3.1 Power spectral density function of the random road profiles

To investigate the vehicle riding characteristics, various forms of ground inputs have been developed. In this work, the ISO road roughness model (Class A-H) is adopted (ISO, 1982). The power spectral density (PSD) function of the ground surface can be expressed as follows:

$$S_g(\Omega)=S_g(\Omega_0)\left(\frac{\Omega}{\Omega_0}\right)^{-N1}, \quad \Omega \le \Omega_0 \tag{4}$$

$$S_g(\Omega)=S_g(\Omega_0)\left(\frac{\Omega}{\Omega_0}\right)^{-N2}, \quad \Omega > \Omega_0 \tag{5}$$

where,

Ω_0 : the reference spatial frequency, $1/2\pi$ (cycles/m)

$S_g(\Omega_0)$: degree of roughness (cycles/m)

$N_1 = 2$

$N_2 = 1.5$

Ω : spatial frequency(cycles/m)

The values of $S_g(\Omega_0)$ (ISO, 1982) for different classes of road are listed in Table 1. It is more convenient to express the PSD function of the ground profile as the function of temporal frequency in hertz for vehicle vibration analysis. The spatial frequency Ω in cycles/m can be transformed to the temporal frequency f in hertz as follows:

$$f = \Omega v \tag{6}$$

where v is the vehicle speed in m/s. Therefore, the PSD function of ground profile can also be transformed and expressed in terms of the temporal frequency f as follows:

$$S_g(f) = S_g(\Omega) = S_g\left(\frac{f}{v}\right) \tag{7}$$

Table 1 Road roughness proposed by ISO (ISO, 1982)

Degree of roughness, $S_g(\Omega_0)$, $10^{-6}m^2$ / cycles / m		
Road Class	Range	Geometric Mean
A (Very Good)	<8	4
B (Good)	8-32	16
C (Average)	32-128	64
D (Poor)	128-512	256
E(Very Poor)	512-2048	1024
F	2048-8192	4096
G	8192-32768	16384
H	>32768	

3.2 Determination of input power spectral density matrix $[S_{xx}(f)]$

The ground profile inputs, $x_1(t)$, $x_2(t)$, $x_3(t)$ and $x_4(t)$, hold on the relationships for the vehicle running at a constant speed v

$$x_1(t) = x_2(t + t_{d1}) \tag{8}$$

$$x_1(t) = x_3(t + t_{d2}) \tag{9}$$

$$x_1(t) = x_4(t + t_{d3}) \tag{10}$$

where

$$t_{d_1} = \frac{l_1 + l_2}{v} \tag{11}$$

$$t_{d_2} = \frac{l_1 + l_2 + l_5 + l_6 + l_8 - l_3}{v} \tag{12}$$

$$t_{d_3} = \frac{l_1 + l_2 + l_5 + l_6 + l_8 + l_4}{v} \tag{13}$$

In which t_{d1} is the delay time between the front wheel of the tractor and the rear wheels of the tractor; t_{d2} is the delay time between the front wheel of the tractor and the front wheel of the trailer; and t_{d3} is the delay time between the front wheel of the tractor and rear wheel of the trailer; therefore, the input spectral density matrix $[S_{xx}(f)]$ can be obtained as follows:

$$[S_{xx}(f)] = S_g(f)\begin{bmatrix} 1 & e^{-j2\pi f t_{d_1}} & e^{-j2\pi f t_{d_2}} & e^{-j2\pi f t_{d_3}} \\ e^{j2\pi f t_{d_1}} & 1 & e^{-j2\pi f (t_{d_2} - t_{d_1})} & e^{-j2\pi f (t_{d_3} - t_{d_1})} \\ e^{j2\pi f t_{d_2}} & e^{j2\pi f (t_{d_2} - t_{d_1})} & 1 & e^{-j2\pi f (t_{d_3} - t_{d_2})} \\ e^{j2\pi f t_{d_3}} & e^{j2\pi f (t_{d_3} - t_{d_1})} & e^{j2\pi f (t_{d_3} - t_{d_2})} & 1 \end{bmatrix} \tag{14}$$

where $S_g(f)$ is the auto-power spectral density function of x_1 and can be substituted by $S_g(f)$ shown in Equation (7).

4 Frequency domain analysis

4.1 Determination of system transfer function matrix $[H_{xy}(f)]$

The equations of motion shown in Equation (1) can take the Laplace transform and become

$$\left([M]s^2 + [C]s + [K]\right)\{Y(s)\} = \left([C']s + [K']\right)\{X(s)\} \tag{15}$$

Let

$$[G(s)] = [M]s^2 + [C]s + [K] \tag{16}$$

and

$$[P(s)] = [C']s + [K'] \tag{17}$$

then

$$[G(s)]\{Y(s)\} = [P(s)]\{X(s)\} \tag{18}$$

$$\{Y(s)\} = [G(s)]^{-1}[P(s)][X(s)] = [H_{xy}(s)]^T\{X(s)\} \tag{19}$$

where

$$[G(s)]^{-1}[P(s)] = [H_{xy}(s)]^T \tag{20}$$

one can easily replace s by $j\omega$ $(= j2\pi f)$, such that

$$\{Y(f)\} = [H_{xy}(f)]^T\{X(f)\} \tag{21}$$

4.2 PSD of system output $[S_{yy}(f)],[S_{xy}(f)]$

From the definition of spectral density matrices, one can obtain

$$[S_{yy}(f)]=[H_{xy}(f)]^{T*}[S_{xx}(f)][H_{xy}(f)] \tag{22}$$

The PSD matrix of output parameters can be determined from the system transfer function and the PSD matrix of input parameters. Similarly, one can get

$$[S_{xy}(f)]=[H_{xy}(f)]^{T}[S_{xx}(f)] \tag{23}$$

It should be noted that $[S_{xx}(f)]$ is the PSD matrix of the ground input defined in Equation (14), and $[H_{xy}(f)]$ is the system transfer function as defined in Equation (20).

4.3 Ride quality parameters

4.3.1 Driver seat acceleration

The spectral density function of the driver seat whose response coordinate is y_6 can be obtained as follows:

$$S_{\ddot{y}_6\ddot{y}_6}=(2\pi f)^4 S_{y_6y_6} \tag{24}$$

where $S_{y_6y_6}$ is the 6th row and 6th column element of $[S_{yy}(f)]$ defined in Equation (22).

4.3.2 Suspension travel

The suspension travels of the front and rear suspensions of the tractor and trailer can be obtained as follows:

$$\delta_1(t)=y_3(t)+l_1y_4(t)-y_1(t) \tag{25}$$

$$\delta_2(t)=y_3-l_2y_4(t)-y_2(t) \tag{26}$$

$$\delta_3(t) = y_5(t)+l_5y_7(t)+(l_5+l_6)\,y_8(t)+(l_8-l_3)\,y_9(t)-y_3(t) \tag{27}$$

$$\delta_4(t) = y_5(t)+l_2y_7t)+(l_5+l_6)\,y_8(t)+(l_8+l_3)\,y_9(t)-y_4(t) \tag{28}$$

The spectral density functions of the front and rear suspension travels of the tractor/trailer can then be derived.

$$S_{\delta_1\delta_1}=S_{y_5y_5}-l_1S_{y_7y_5}-S_{y_1y_5}-l_1S_{y_5y_7}+l_1^2S_{y_7y_7}+l_1S_{y_1y_7}-S_{y_5y_1}+l_1S_{y_7y_1}+S_{y_1y_1} \tag{29}$$

$$S_{\delta_2\delta_2}=S_{y_5y_5}+l_2S_{y_7y_5}-S_{y_2y_5}+l_2S_{y_5y_7}+l_2^2S_{y_7y_7}-l_2S_{y_2y_7}-S_{y_5y_2}-l_2S_{y_7y_2}+S_{y_2y_2} \tag{30}$$

$$\begin{aligned}S_{\delta_3\delta_3}=&S_{y_5y_5}+l_7S_{y_7y_5}+(l_5+l_6)S_{y_8y_5}+(l_8-l_3)S_{y_9y_5}-S_{y_3y_5}+l_7S_{y_5y_7}+l_7^2S_{y_7y_7}+l_7(l_5+l_6)S_{y_8y_7}+l_7(l_8-l_3)S_{y_9y_7}\\&-l_7S_{y_3y_7}+(l_5+l_6)S_{y_5y_8}+l_7(l_5+l_6)S_{y_7y_8}+(l_5+l_6)^2S_{y_8y_8}+(l_8-l_3)(l_5+l_6)S_{y_9y_8}-(l_5+l_6)S_{y_3y_8}\\&+(l_8-l_3)S_{y_5y_9}+l_7(l_8-l_3)S_{y_7y_9}+(l_5+l_6)(l_8-l_3)S_{y_8y_9}+(l_8-l_3)^2S_{y_9y_9}-(l_8-l_3)S_{y_3y_9}\\&-S_{y_5y_3}-l_7S_{y_7y_3}-(l_5+l_6)S_{y_8y_3}-(l_8-l_3)S_{y_9y_3}+S_{y_3y_3}\end{aligned} \tag{31}$$

$$\begin{aligned}S_{\delta_4\delta_4}=&S_{y_5y_5}+l_7S_{y_7y_5}+(l_5+l_6)S_{y_8y_5}+(l_8+l_4)S_{y_9y_5}-S_{y_4y_5}+l_7S_{y_5y_7}+l_7^2S_{y_7y_7}+l_7(l_5+l_6)S_{y_8y_7}+l_7(l_8+l_4)S_{y_9y_7}\\&-l_7S_{y_4y_7}+(l_5+l_6)S_{y_5y_8}+l_7(l_5+l_6)S_{y_7y_8}+(l_5+l_6)^2S_{y_8y_8}+(l_8+l_4)(l_5+l_6)S_{y_9y_8}-(l_5+l_6)S_{y_4y_8}\\&+(l_8+l_4)S_{y_5y_9}+l_7(l_8+l_4)S_{y_7y_9}+(l_5+l_6)(l_8+l_4)S_{y_8y_9}+(l_8+l_4)^2S_{y_9y_9}-(l_8+l_4)S_{y_4y_9}\\&-S_{y_5y_4}-l_7S_{y_7y_4}-(l_5+l_6)S_{y_8y_4}-(l_8+l_4)S_{y_9y_4}+S_{y_4y_4}\end{aligned} \tag{32}$$

4.3.3 Road holding

The road holdings of the front and rear tyres of the tractor and trailer can be defined as follows:

$$h_1(t)=y_1(t)-x_1(t) \tag{33}$$

$$h_2(t)=y_2(t)-x_2(t) \tag{34}$$

$$h_3(t)=y_3(t)-x_3(t) \tag{35}$$

$$h_4(t)=y_4(t)-x_4(t) \tag{36}$$

when $h_i(t)$ are positive, the wheels and the road remain contact. The spectral density functions of the road holdings can be derived.

$$S_{h_1h_1}=S_{y_1y_1}-S_{y_1x_1}-S_{x_1y_1}+S_{x_1x_1} \tag{37}$$

$$S_{h_2h_2}=S_{y_2y_2}-S_{y_2x_2}-S_{x_2y_2}+S_{x_2x_2} \tag{38}$$

$$S_{h_3h_3}=S_{y_3y_3}-S_{y_3x_3}-S_{x_3y_3}+S_{x_3x_3} \tag{39}$$

$$S_{h_4h_4}=S_{y_4y_4}-S_{y_4x_4}-S_{x_4y_4}+S_{x_4x_4} \tag{40}$$

4.3.4 Dynamic tyre force

The dynamic tyre forces between tyres and the road surface can also be shown as follows:

$$f_1(t)=k_{t_1}h_1(t)+c_{t_1}\dot{h}_1(t) \tag{41}$$

$$f_2(t)=k_{t_2}h_2(t)+c_{t_2}\dot{h}_2(t) \tag{42}$$

$$f_3(t)=k_{t_3}h_3(t)+c_{t_3}\dot{h}_3(t) \tag{43}$$

$$f_4(t) = k_{t_4} h_4(t) + c_{t_4} \dot{h}_4(t) \tag{44}$$

The spectral density functions of contact forces between tyres and road surfaces can be obtained as:

$$S_{f_1 f_1} = \left(k_{t_1}^2 + (2\pi f)^2 c_{t_1}^2\right) S_{h_1 h_1} \tag{45}$$

$$S_{f_2 f_2} = \left(k_{t_2}^2 + (2\pi f)^2 c_{t_2}^2\right) S_{h_2 h_2} \tag{46}$$

$$S_{f_3 f_3} = \left(k_{t_3}^2 + (2\pi f)^2 c_{t_3}^2\right) S_{h_3 h_3} \tag{47}$$

$$S_{f_4 f_4} = \left(k_{t_4}^2 + (2\pi f)^2 c_{t_4}^2\right) S_{h_4 h_4} \tag{48}$$

4.3.5 *Tractor and trailer body acceleration*

$\bar{z}_1 \sim \bar{z}_{12}$ are defined as the locations of tractor/trailer as shown in Figure 2. $\bar{z}_1 \sim \bar{z}_6$ are the locations in the tractor, and $\bar{z}_7 \sim \bar{z}_{12}$ are the locations in the trailer. The $\bar{z}_i$ and its spectral density function can be derived as follows:

1 For i = 1 to 3

$$\bar{z}_i = y_5 - l_{z_i} y_7$$

$$S_{\bar{z}_i \bar{z}_i} = S_{y_5 y_5} - l_{z_i} S_{y_5 y_7} - l_{z_i} S_{y_7 y_5} + l_{z_i}{}^2 S_{y_7 y_7} \tag{49}$$

2 For i = 4 to 6

$$\bar{z}_i = y_5 + l_{z_i} y_7$$

$$S_{z_i z_i} = S_{y_5 y_5} + l_{z_i} S_{y_5 y_7} + l_{z_i} S_{y_7 y_5} + l_{z_i}{}^2 S_{y_7 y_7} \tag{50}$$

3 For i = 7 to 12

$$\bar{z}_i = y_5 + l_7 y_7 + (l_5 + l_6) y_8 + l_{z_i} y_9$$

$$\begin{aligned} S_{z_i z_i} = {} & S_{y_5 y_5} + l_7 S_{y_7 y_5} + (l_5 + l_6) S_{y_8 y_5} + l_{z_i} S_{y_9 y_5} + l_7 S_{y_5 y_7} + l_7{}^2 S_{y_7 y_7} + (l_5 + l_6) S_{y_5 y_8} \\ & + l_7 (l_5 + l_6) S_{y_7 y_8} + (l_5 + l_6)^2 S_{y_8 y_8} + l_{z_i} (l_5 + l_6) S_{y_9 y_8} + l_{z_i} S_{y_5 y_9} + l_7 l_{z_i} S_{y_7 y_9} \\ & + (l_5 + l_6) l_7 S_{y_8 y_7} + l_7 l_{z_i} S_{y_9 y_7} + (l_5 + l_6) l_{z_i} S_{y_8 y_9} + l_{z_i}{}^2 S_{y_9 y_9} \end{aligned} \tag{51}$$

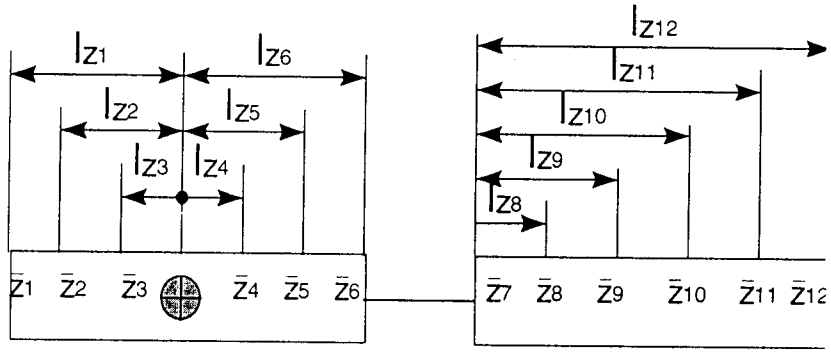

Figure 2 *Definition of* $\bar{z}_1 \sim \bar{z}_{12}$.

4.4 *RMS Acceleration in 1/3 octave band*

The PSD function of the acceleration can be obtained from the PSD function of the displacement as follows:

$$S_{\ddot{y}\ddot{y}}(f) = (2\pi f)^4 S_{yy}(f) \tag{52}$$

where $S_{\ddot{y}\ddot{y}}(f)$ is the PSD function of acceleration. The RMS (root mean square) acceleration at a given centre frequency f_c in 1/3 octave band can be determined by:

$$\ddot{y}_{1/3\text{-}RMS} = \left[\int_{f_l}^{f_u} S_{\ddot{y}\ddot{y}}(f)\,df\right]^{\frac{1}{2}} \tag{53}$$

where

$f_u = 2^{1/6} f_c$ upper band frequency

$f_l = 2^{-1/6} f_c$ lower band frequency

$\ddot{y}_{1/3\text{-}RMS}$: RMS acceleration in 1/3 octave band

f_c : central frequency

The upper central frequency is $2^{1/3}$ times the lower. The RMS values of vertical accelerations at the driver's seat in 1/3 Octave Band can be computed and compared with the reduced comfort boundaries recommended by ISO 2631 (ISO, 1978) to evaluate the ride comfort

4.5 Standard deviation of the ride quality parameters

The standard deviation of the ride quality parameters acceleration can also be obtained for zero mean values as follows:

$$\sigma_z = \left[\int_{f_l}^{f_u} S_{zz}(f) df \right]^{\frac{1}{2}} \tag{54}$$

where z is any of the ride quality parameters; $S_{zz}(f)$ is the PSD function of z; and σ_z denotes the standard deviation of z.

5 Results and discussion

A conventional truck and full trailer, whose values and units are listed in Appendix B, is adopted for the following analytical simulation. Firstly, the characteristics of the system transfer functions are studied. The RMS acceleration of the driver seat in the 1/3 octave band is then compared with the ISO 2631 ride comfort criteria (ISO, 1978). The characteristics of the ride quality parameters, including the suspension travels, road holdings and dynamic tyre forces, are also studied. Finally, the acceleration response over the tractor and trailer are presented and can be utilized to evaluate the ride quality of the cargo. In the following simulation analysis, different vehicle speeds, road surface conditions and laden conditions are considered. It is noted that the suspension and tyre parameters are not optimum in this paper.

5.1 Characteristics of transfer functions

Table 2 shows the natural frequencies of the system considering the half/half laden conditions, i.e., half-laden in the tractor and half-laden in the trailer. Four natural frequencies near 5 Hz can be recognized as the unsprung mass natural frequencies. The others are then related to the sprung mass units, including the driver seat, draw bar, the tractor and the trailer.

Table 2 Natural frequencies of the system (laden half/half).

Mode	*Natural frequency (Hz)*
1	0.59224
2	0.60378
3	0.91372
4	1.03360
5	1.07027
6	5.28198
7	5.28208
8	5.28769
9	5.28919

The system transfer functions between the input and output coordinates can be derived as shown in Equation (20). Figure 3 shows the amplitudes of the system transfer functions for the half/half laden condition. Figures 3(a)-3(d) represent the transfer functions between the tyre/road contact points and the unsprung mass units (wheel axles). For H_{ii}, i = 1,2,3,4, the transfer functions are similar, because they are transfer functions between the tyres and their wheel axle. Figures 3(a) and 3(b) for the tractor are similar, and Figures 3(c) and 3(d) for the trailer are also similar.

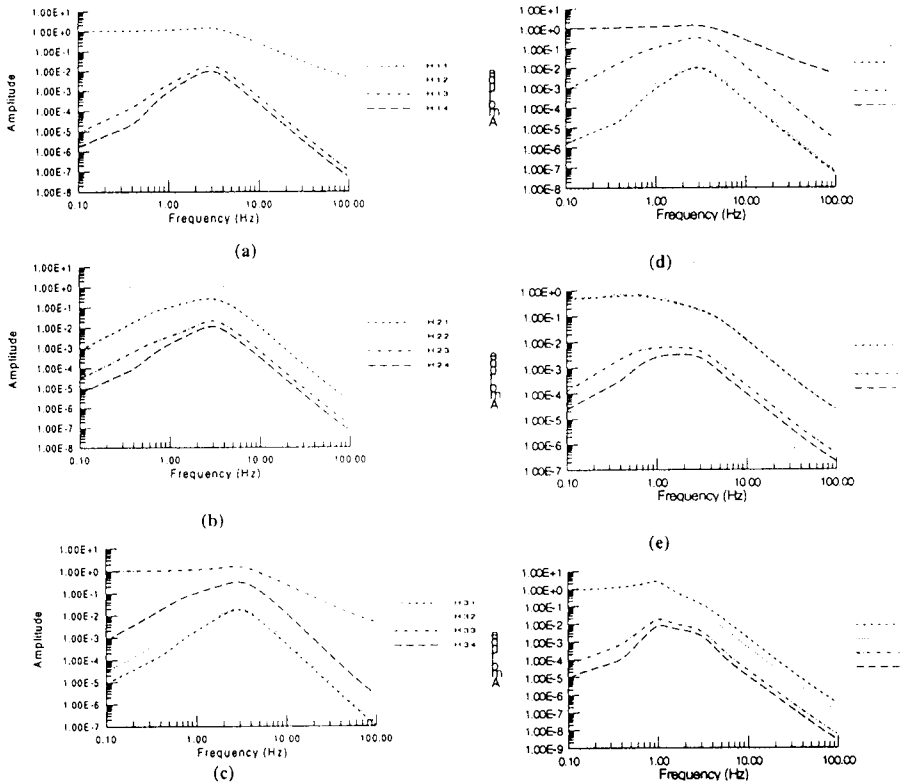

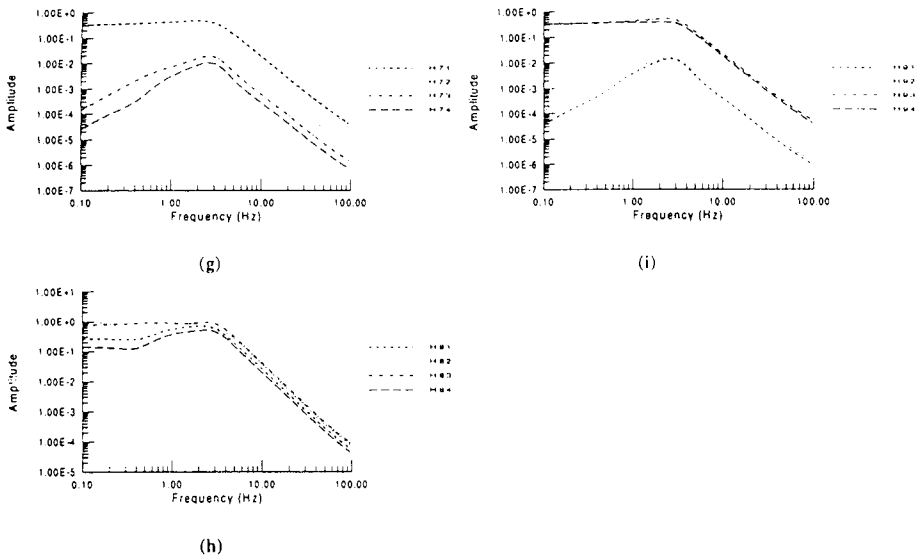

Figure 3 *Transfer functions for the 9 DOF truck and full trailer.*

From Figure 3(e), one can see that the amplitudes of H_{51} and H_{52} are close to each other, i.e., the vertical response of the tractor due to its two wheel set inputs is about the same. The amplitudes of H_{53} and H_{54} are much smaller than H_{51} and H_{52}. It can be seen that the tractor response is more influenced by the first and second wheel axles than by the third and fourth wheel axles.

As shown in Figure 3(f), the amplitudes of H_{61} and H_{62} are larger than those of H_{63} and H_{64}, i.e., the driver's seat response is dominantly influenced by the tractor wheel axles. As seen in Figure 3(g), the amplitudes of H_{61} and H_{62} are larger than those of H_{63} and H_{64}, i.e., the pitch response of the tractor is mainly influenced by the tractor wheel axles. The pitch response of the tractor due to the first and second wheel axles can be about the same, because of the closeness of the amplitudes of H_{61} and H_{62}.

As shown in Figure 3(h), the amplitudes of H_{82} and H_{83} are larger than those of H_{81} and H_{84}, especially for frequencies below 1 Hz. As expected, the draw bar is mainly influenced by the second and third wheel axles.

From Figure 3(i), the amplitudes of H_{93} and H_{94} are higher than those of H_{91} and H_{92}, i.e., the trailer response is dominated by the third and fourth wheel axle inputs.

From the observation of transfer functions, their characteristics can be summarized as follows:

1 The response of each unsprung mass is dominated by its own wheel axle input.

2 The driver seat response is dominated by the first and second wheel axle inputs.

3 The vertical and pitch response of the tractor are dominantly influenced by the first and second wheel axle inputs.

4 The draw bar response is dominated by the second and third wheel axle inputs.

5 The tractor response is dominated by the third and fourth wheel axle inputs.

5.2 The assessment of ride quality

5.2.1 The ride comfort of the driver

Figure 4(a) shows the RMS accelerations of the driver seat in the 1/3 octave band for different vehicle speeds (60, 75, 90 and 100 km/hr), when the road surface is assumed to be ISO road class B (good), and the laden condition is half-laden for the tractor and half-laden for the trailer. The ISO comfort criteria for 1-hour and 8-hour are also plotted. One can see that the ride comfort of the driver can be quite good at different vehicle speeds. Changing the vehicle's speed does not affect the driver's comfort very much.

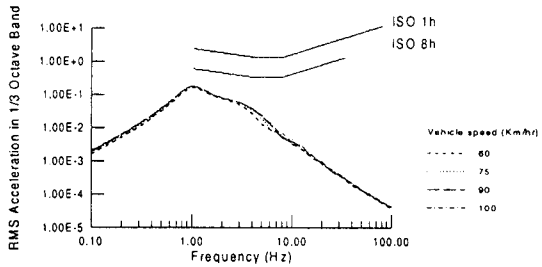

(a) Vehicle speed (ISO road class B, Laden condition half/half)

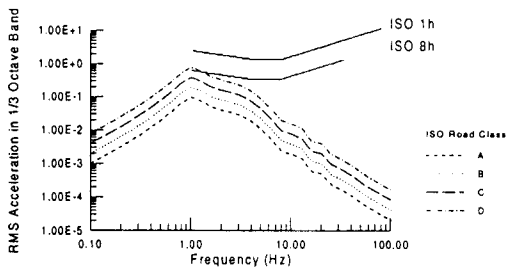

(b) ISO road class (Vehicle speed 90 km/hr, Laden condition half/half)

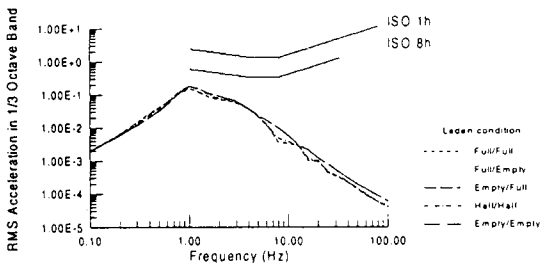

(c) Laden condition (ISO road class B, Vehicle speed 90 km/hr

Figure 4 *RMS acceleration of driver-seat in 1/3 octave band.*

The standard deviations of the acceleration of the driver seat calculated based on Equation (54) for different vehicle speeds are also listed in Table 3(a). As expected, the higher the vehicle speed, the higher the standard deviation.

Table 3 Standard deviation of driver seat acceleration.

(a) Vehicle speed (ISO road class: B, Laden half/half)

Speed (km/hr)	*60*	*75*	*90*	*100*
$\sigma_{\ddot{y}_6}\ (m/\sec^2)$	0.28113	0.30550	0.32429	0.33523

(b) Road (Vehicle speed 90 km/hr, Laden condition half/half)

ISO Road Class	*A(Very Good)*	*B(Good)*	*C(Average)*	*D(Poor)*
$\sigma_{\ddot{y}_6}\ (m/\sec^2)$	0.16214	0.32129	0.64858	1.29716

(c) Laden (ISO road class: B, Vehicle speed 90 km/hr)

Laden (Tractor/ Trailer)	*Full/Full*	*Full/Empty*	*Empty/Full*	*Half/Half*	*Empty/Empty*
$\sigma_{\ddot{y}_6}\ (m/\sec^2)$	0.27562	0.27715	0.32528	0.32429	0.32594

(d) Laden (ISO road class: B, Vehicle speed 90 km/hr)

Laden(Tractor/Trailer)	*Full/Full*	$r_{w_1} = 0.7$ / $r_{w_2} = 0.7$	*Half/Half*	$r_{w_1} = 0.2$ / $r_{w_2} = 0.2$	*Empty/Emp*
$\sigma_{\ddot{y}_6}\ (m/\sec^2)$	0.27562	0.30406	0.32429	0.33059	0.32549

Table 4 Standard deviation of suspension travel

(a) Vehicle speed (ISO road class: B, Laden half/half)

Speed (km/hr)	*60*	*75*	*90*	*100*
σ_{d_1} (m)	0.00370	0.00423	0.00464	0.00487
σ_{d_2} (m)	0.00321	0.00366	0.00408	0.00434
σ_{d_3} (m)	0.00349	0.00400	0.00440	0.00464
σ_{d_4} (m)	0.00325	0.00368	0.00409	0.00435

(b) Road (Vehicle speed 90 km/hr, Laden condition half/half)

ISO Road Class	*A(Very Good)*	*B(Good)*	*C(Average)*	*D(Poor)*
σ_{d_1} (m)	0.00232	0.00464	0.00928	0.01857
σ_{d_2} (m)	0.00204	0.00408	0.00816	0.01631
σ_{d_3} (m)	0.00220	0.00440	0.00881	0.01762
σ_{d_4} (m)	0.00204	0.00409	0.00818	0.01636

(c) Laden (ISO road class: B, Vehicle speed 90 km/hr)

Laden(Tractor/ Trailer)	*Full/Full*	*Full/Empty*	*Empty/Full*	*Half/Half*	*Empty/Empty*
σ_{d_1} (m)	0.00564	0.00566	0.00288	0.00464	0.00289
σ_{d_2} (m)	0.00519	0.00517	0.00316	0.00408	0.00315
σ_{d_3} (m)	0.00529	0.00277	0.00530	0.00440	0.00276
σ_{d_4} (m)	0.00534	0.00296	0.00534	0.00409	0.00296

Figure 4(b) shows the RMS accelerations of the driver seat in the 1/3 octave band for different road surfaces (ISO road classes A, B, C and D), when the vehicle speed is assumed to be 90 km/hr, and the laden condition is half-laden for the tractor and half-laden for the trailer. The driver's ride quality is within the ISO 2631 8-hour comfort limit except for the ISO road class D (poor). For different classes of road conditions, the RMS acceleration varies largely as expected, because the road surfaces are defined by ISO 2631 (1978) which characterizes the different classes of the road roughness in a large scale of order. The standard deviations of the driver seat are tabulated in Table 3(b). The better the road conditions, the lower the standard deviations.

Figure 4(c) shows the RMS accelerations of the driver seat in 1/3 octave band for different laden conditions, such as Full/Full, Full/Empty, Empty/Full, Half/Half and Empty/Empty, when the vehicle speed is assumed to be 90 km/hr, and the ISO road class is B (good). The driver's ride comfort is not much influenced by the laden conditions. However, as shown in Table 3(c) the standard deviation of driver seat acceleration is larger for the Empty/Empty laden condition than for others. It is also interesting to note that the Full/Empty laden condition will provide better ride quality for the driver than the Empty/Full laden condition, and the Half/Half laden condition is just somewhere in between the Full/Empty and the Empty/Full laden conditions.

5.2.2 *Suspension travel*

Table 4(a) shows the standard deviations of suspension travels for the four wheel sets, corresponding to the cases shown in Figure 4(a). For purposes of comparison, the standard deviations of suspension travels are also plotted in Figure 5(a). One can see that the standard deviations of the front suspension travels for the front wheel axles of the tractor and trailer are higher than the rear axles. As the increase of the vehicle speed, the standard deviation of the suspension travel can be expected to be higher.

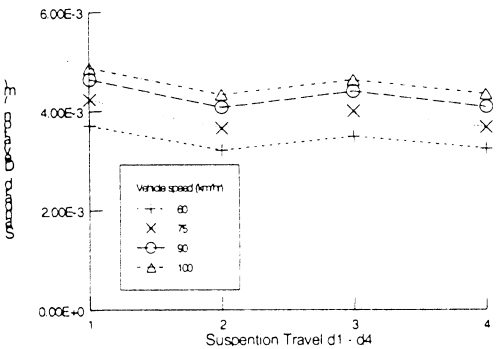

(a) Vehicle speed (ISO road class B, Laden condition half/half)

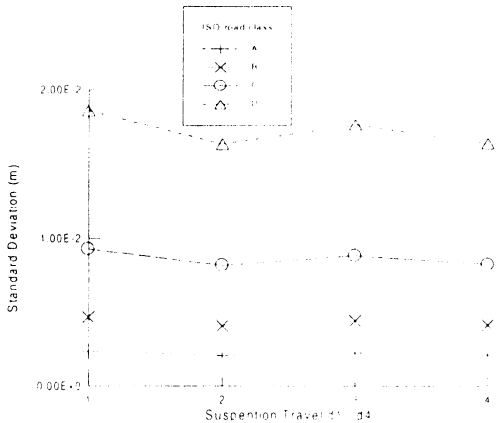

(b) ISO road class (Vehicle speed 90 km/hr, Laden condition half/half)

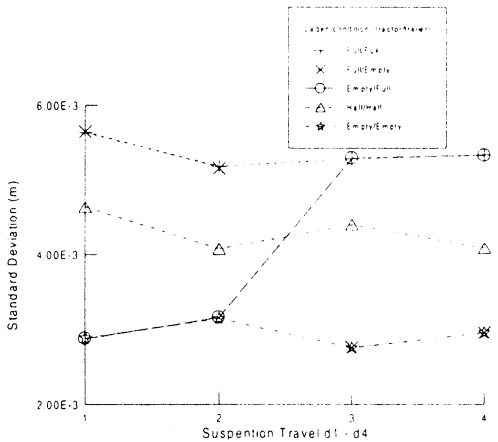

(c) Laden(ISO road class B, Vehicle speed 90 km/hr)

Figure 5 *Standard deviation of suspension travel.*

Table 4(b) shows the standard deviations of suspension travels for the four wheel sets, corresponding to the cases shown in Figure 4(b). The standard deviations of the suspension travel are also plotted in Figure 5(b). As one can see, the better the road surface condition, the lower the standard deviations of the suspension travel. Again, the front wheel axles of the trailer experience higher suspension travels than the rear ones for either the tractor or trailer.

Table 4(c) shows the standard deviations of suspension travels for the four wheel axles, corresponding to the cases shown in Figure 4(c). The standard deviations of the

suspension travel are also plotted in Figure 5(c). As expected, the higher the laden, the higher the standard deviations of the suspension travels. In particular, the standard deviations of the suspension travels for the case of Half/Half condition is just somewhere in between the Full/Full and Empty/Empty laden conditions.

Table 5 Standard deviation of road holding.

(a) Vehicle speed (ISO road class: B, Laden half/half)

Speed (km/hr)	*60*	*75*	*90*	*100*
σ_{h_1} (m)	0.00292	0.00325	0.00349	0.00361
σ_{h_2} (m)	0.00268	0.00287	0.00304	0.00314
σ_{h_3} (m)	0.00301	0.00335	0.00359	0.00372
σ_{h_4} (m)	0.00270	0.00288	0.00303	0.00313

(b) Road (Vehicle speed 90 km/hr, Laden half/half)

ISO Road Class	*A(Very Good)*	*B(Good)*	*C(Average)*	*D(Poor)*
σ_{h_1} (m)	0.00174	0.00349	0.00698	0.01396
σ_{h_2} (m)	0.00152	0.00304	0.00608	0.01216
σ_{h_3} (m)	0.00179	0.00359	0.00718	0.01436
σ_{h_4} (m)	0.00152	0.00303	0.00606	0.01212

(c) Laden (ISO road class: B, Vehicle speed 90 km/hr)

Laden(Tractor/ Trailer)	*Full/Full*	*Full/Empty*	*Empty/Full*	*Half/Half*	*Empty/Empty*
σ_{h_1} (m)	0.00352	0.00352	0.00330	0.00349	0.00330
σ_{h_2} (m)	0.00303	0.00303	0.00323	0.00304	0.00323
σ_{h_3} (m)	0.00361	0.00339	0.00361	0.00359	0.00339
σ_{h_4} (m)	0.00303	0.00324	0.00303	0.00303	0.00324

5.2.3 *Road holding*

Figures 6(a)-6(c) show the standard deviations of the road holdings corresponding to the cases in Figures 4(a)-4(c). The values of the standard deviations of the road holdings are listed in Table 5(a)-5(c). As shown in Figure 6(a), the front tyres of the tractor and

trailer have higher standard deviations of the road holding than the rear ones. The smaller the standard deviation of road holding, the better the road holding ability. As the increase of the vehicle speed, the chance of the departure of the tyre from the road is increased.

From Figure 6(b), the worse the road condition, the worse the road holding. For equally loaded conditions as shown in Figure 6(c), the front tyres of the tractor and trailer have the higher standard deviation of road holding. As the increase of the loading, the standard deviation of the road holding for the front tyres are increased; however, those for the rear tyres are decreased.

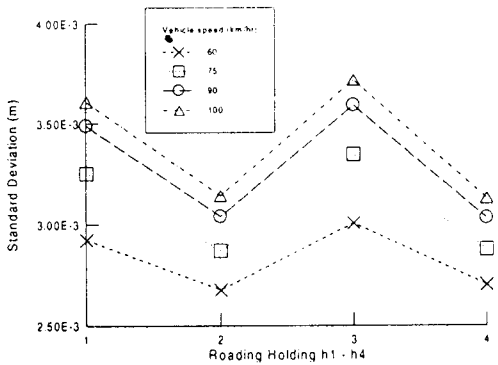

(a) Vehicle speed (ISO road class B, Laden condition half/half)

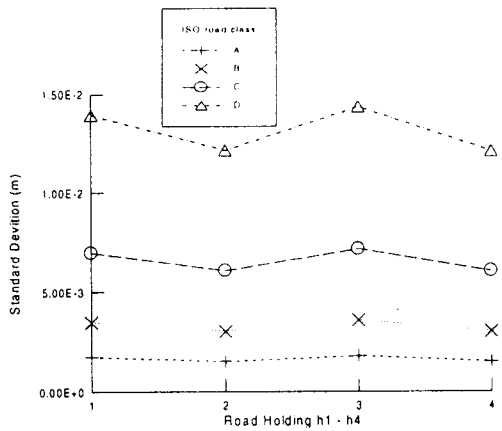

(b) ISO road class (Vehicle speed 90 km/hr, Laden condition half/half)

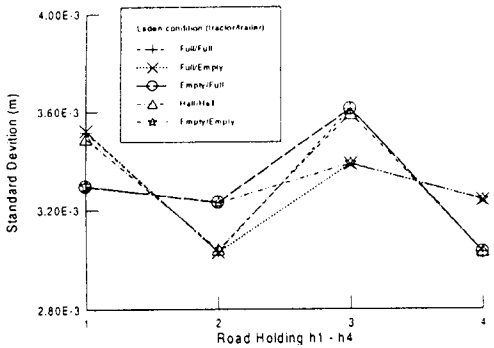

(c) Laden condition (ISO road class B, Vehicle speed 90 km/hr)

Figure 6 *Standard deviation of road holding.*

5.2.4 dynamic tyre force

The dynamic tyre forces are directly related to the road holding, as shown in Equations (37)-(40). Figures 7(a)-7(c) and Table 6(a)-6(c) are corresponding to the cases in Figures 6(a)-6(c) and Table 5(a)-5(c), respectively. From the observation of Figures 7(a)-7(c), the higher the vehicle speed, the higher the tyre force; the worse the road condition, the higher the tyre force. The front tyres of the tractor and trailer generally have higher tyre force than the rear. As the increase of the loading, the front tyre forces increase; however, the rear tyre forces decrease. The tyre wears in the first and third wheel axles can be excepted higher than those in the second and fourth.

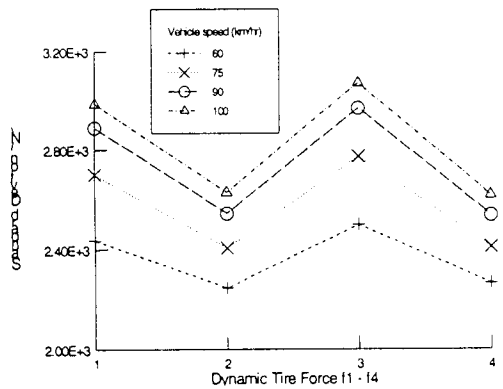

(a) Vehicle speed (ISO road class B, Laden condition half/half)

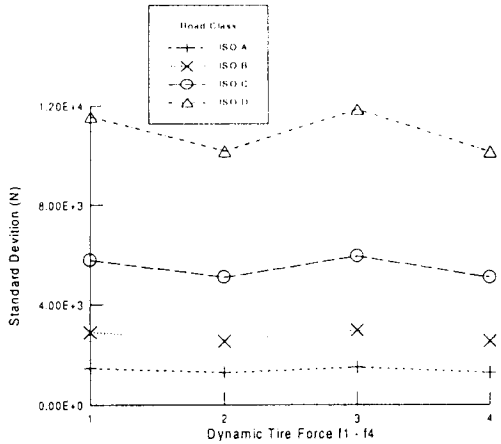

(b) ISO road class(Vehicle speed 90 km/hr, Laden condition half/half)

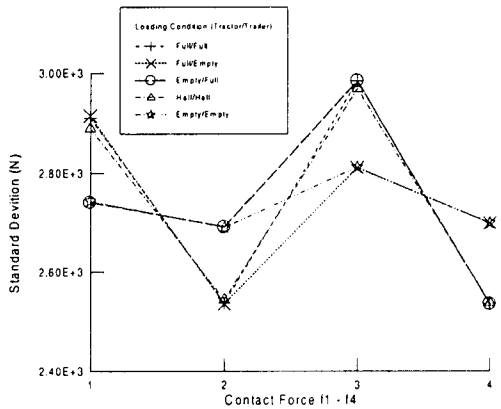

(c) Laden condition (ISO road class B, Vehicle speed 90 km/hr)

Figure 7 *Standard deviation of contact forces between tyre/road.*

Table 6 Standard deviation of dynamic tyre force.

(a) Vehicle speed (ISO road class: B, Laden condition half/half)

Speed (km/hr)	*60*	*75*	*90*	*100*
σ_{f_1} (N)	2435.36	2700.37	2890.16	2986.81
σ_{f_2} (N)	2245.30	2404.72	2544.66	2628.82
σ_{f_3} (N)	2498.39	2773.15	2968.41	3070.61
σ_{f_4} (N)	2264.19	2408.60	2537.13	2617.72

(b) Road (Vehicle speed 90 km/hr , Laden half/half)

ISO Road Class	*A(Very Good)*	*B(Good)*	*C(Average)*	*D(Poor)*
σ_{f_1} (N)	1445.08	2890.16	5780.31	11560.63
σ_{f_2} (N)	1272.33	2544.66	5089.32	10178.65
σ_{f_3} (N)	1484.20	2968.41	5936.81	11873.62
σ_{f_4} (N)	1268.56	2537.13	5074.26	10148.51

(c) Laden (ISO road class: B, Vehicle speed condition 90 km/hr)

Laden (Tractor/ Trailer)	*Full/Full*	*Full/Empty*	*Empty/Full*	*Half/Half*	*Empty/Empty*
σ_{f_1} (N)	2910.33	2914.70	2741.11	2890.16	2743.51
σ_{f_2} (N)	2536.76	2535.23	2691.13	2544.66	2689.67
σ_{f_3} (N)	2984.07	2810.64	2984.46	2968.41	2811.69
σ_{f_4} (N)	2535.10	2698.07	2535.05	2537.13	2698.00

5.5.5 *The tractor and trailer body acceleration*

The standard deviations of the accelerations of $\ddot{z}_1$-$\ddot{z}_{12}$ which are defined as shown in Figure 2. Figures 8(a)-8(d) are shown for the effects of different vehicle speeds, different road conditions and different laden conditions, respectively. In general, the standard deviations of the accelerations at the centre of gravity of the tractor and trailer are smaller than elsewhere. The standard deviation of the trailer body acceleration is slightly higher than that of the tractor. The effect of vehicle speed and road condition are significant. As expected, the higher the vehicle speed, and the worse the road

condition, the worse the ride quality of the cargo. For better ride quality of the cargo, the cargo should be placed on the tractor in preference to on the trailer. The cargo should be placed as near as possible to the centre of gravity of the tractor or trailer for better ride quality of the cargo.

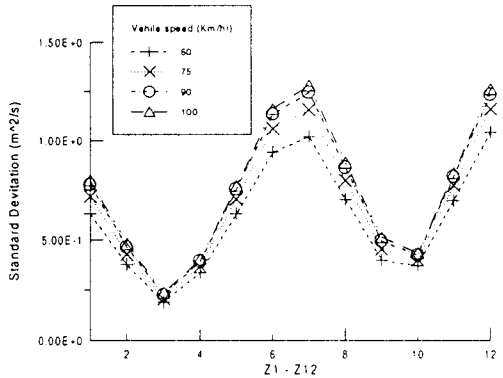

(a) Vehicle speed (ISO road class B, Laden condition half/half)

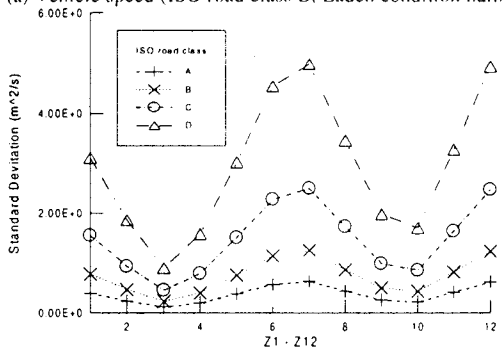

(b) ISO road class(Vehicle speed 90 km/hr, Laden condition half/half)

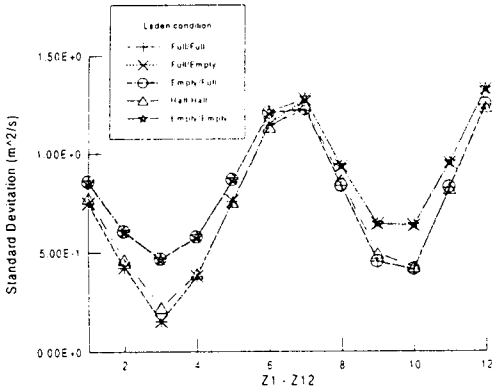

(c) Laden condition (ISO road class B, Vehicle speed 90 km/hr)

Figure 8 *Standard deviation of tractor and trailer body acceleration.*

6 Conclusions

This paper shows the ride quality analysis of the truck and full trailer. The 9 DOF riding model is first developed. The tractor and trailer are assumed to be rigid bodies subjected to the vertical and pitch motion only. The suspension system and tyres are modelled to be linear spring-damper elements. The model is also assumed to be symmetric along the moving direction. The displacement input of stationary ergodic Gaussian random road surface defined by ISO is adopted in this work. The frequency response functions (transfer functions) can be defined between the input and output vectors of the linear system. Therefore, the output power spectral density (PSD) function of the system related to the PSD function of the road input can be determined through the frequency domain analysis. As the output PSD functions for the accelerations of the vehicle have been obtained, the root-mean square values of acceleration as a function of frequency in 1/3 octave band can be obtained. Finally, the riding quality of the driver seat can be evaluated in comparison to the ISO 2631 vertical acceleration spectra. The system parameters, including suspension travel, road holding and dynamic tyre load between the tyre and the road are also studied. They are important factors for the design of the tractor and trailer system. The results can be used for further analysis, such as the evaluation of the cargo ride quality and road damage. The developed model can also be utilized for the optimum design of system variables.

Acknowledgement

The authors gratefully acknowledge the support of the work by National Science Council, Republic of China, under grant NSC 84-2212-E-020-009.

References

Atalik, T. S., and S. Utku, (1976) 'Stochastic linearization of multi-degree of-freedom non-linear systems,' *Earthquake Engineering and Structural Dynamics*, Vol. 4, pp. 411-420.

Bendat, J. S., (1986) *Random Data Analysis and Measurement Procedures*, 2nd ed., John Wiley & Sons, Inc.

Clark, S. K.(ed), (1981) 'Mechanics of pneumatic tires,' *US Department of Transportation*, NHTSA, DOT HS 805952.

Dahlberg, T., (1979) 'An optimized speed-controlled suspension of a 2-DOF vehicle traveling on a randomly profiled road,' *Journal of Sound and Vibration*, Vol. 62, pp. 541-546.

Demic, M., (1992) 'Optimization of characteristics of elasto-damper elements of cars from the aspect of comfort and handling,' *Int. J. of Vehicle Design*, Vol. 13, No. 1, pp. 29-46.

Del Castillo, J., M. P. Pintado, and F. G. Benitez, (1990) 'Optimization for vehicle suspension II: frequency domain,' *Vehicle System Dynamics*, Vol. 19, pp. 331-352.

Dohi, M., and Y. Maruyama, (1990) 'Ride Comfort Optimization for Commercial Trucks,' *SAE Transaction*, Vol. 99, No. 2, pp. 890-902.

ElMadany, M. M., (1987) 'A procedure for optimization of truck suspension,' *Vehicle System Design*, Vol. 16, pp. 297-312.

ElMadany, M. M., and M. A. Dokainish, (1980) 'Articulated vehicle dynamic analysis using equivalent linearization technique,' *SAE Transactions*, Vol. 89, Report 801421, pp. 4506-4517.

ElMadany, M. M., and Z. Abduljabbar, (1990) 'Design evaluation of advanced suspension systems for truck ride comfort,' *Computers & Structures*, Vol. 36, No. 2, pp. 321-331.

Hac, A., (1985) 'Suspension optimization of a 2-DOF vehicle model using a stochastic optimal control technique,' *Journal of Sound and Vibration*, Vol. 100, pp. 343-357.

ISO, (1978) 'Guide for the evaluation of human exposure to whole-body vibration,' 2nd edn., International Standard 2631-1978(E), *International Organization for Standardization.*

ISO, (1982) 'Reporting vehicle road surface irregularities,' ISO/TC108/SC2/WG4 N57.

Iwan, W. D., and I. M. Yang, (1972) 'Application of statistical linearization techniques to nonlinear multi-degree of freedom systems,' *Journal of applied Mechanics*, Vol. 39, pp. 545-550.

Lee, R., and F. Pradko, (1968) 'Analytical analysis of human vibration,' *SAE Transaction*, Report No. 680091, pp. 346-370.

Ravalard, Y., D. Coutellier, and S. Masfrand, (1994) 'Dynamic behavior of articulated train car and influence on vertical comfort,' *Transaction of CSME*, Vol. 18, No. 3, pp. 269-283.

Ryba, D., (1974) 'Improvement in dynamic characteristics of automobile suspension systems, Part 1. Two Mass System,' *Vehicle System Dynamics*, Vol. 3, pp. 17-46.

Sun, J., (1987) 'Frequency spectral analysis of bridge-vehicle system due to road surface roughness,' *Vehicle System Dynamics*, Vol. 16, pp. 227-239.

Stikeleather, L. F., (1976) 'Review of ride vibration standards and tolerance criteria,' *SAE Transaction*, Report No. 760413, pp. 1460-1467

Vaduri, S., and E. H. Law, (1993) 'Development of a simulation for assessment of ride quality of tractor and trailer,' *SAE* Report 932940.

Margolis, D., and D. Edeal, (1989) 'Modeling and control of large flexible frame vehicles using bond graphics,' *SAE* Report 892488.

Pintado, P., and F. G. Benitez, (1990) 'Optimization for vehicle suspension II: time domain,' *Vehicle System Dynamics*, Vol. 19, pp. 273-288.

Appendix A: Definition of system matrices

$$[M]=\begin{bmatrix}
m_1 & 0 & 0 & 0 & 0 & 0 & 0 & 0 & 0\\
0 & m_2 & 0 & 0 & 0 & 0 & 0 & 0 & 0\\
0 & 0 & m_3 & 0 & 0 & 0 & 0 & 0 & 0\\
0 & 0 & 0 & m_4 & 0 & 0 & 0 & 0 & 0\\
0 & 0 & 0 & 0 & m_5+\frac{m_6 l_6}{l_5+l_6} & 0 & \frac{m_6 l_6 l_7}{l_5+l_6} & \frac{m_6 l_5 l_6-l_6}{l_5+l_6} & 0\\
0 & 0 & 0 & 0 & m_7+\frac{m_6 l_5}{l_5+l_6} & 0 & m_7 l_7+\frac{m_6 l_5 l_7}{l_5+l_6} & m_7(l_5+l_6)+\frac{m_6 l_5^2+l_6}{l_5+l_6} & m_7 l_8\\
0 & 0 & 0 & 0 & 0 & m_8 & 0 & 0 & 0\\
0 & 0 & 0 & 0 & \frac{m_6 l_6 l_7}{l_5+l_6} & 0 & I_5+\frac{m_6 l_6 l_7^2}{l_5+l_6} & \frac{m_6 l_5 l_6 l_7-l_6 l_7}{l_5+l_6} & 0\\
0 & 0 & 0 & 0 & -\frac{m_6 l_5 l_8}{l_5+l_6} & 0 & -\frac{m_6 l_5 l_7 l_8}{l_5+l_6} & -\frac{I_6 l_8+m_6 l_5^2 l_8}{l_5+l_6} & I_7
\end{bmatrix}$$

$$[C]=\begin{bmatrix}
c_{s_1}+c_{t_1} & 0 & 0 & 0 & -c_{s_1} & 0 & c_{s_1}l_1 & 0 & 0\\
0 & c_{s_2}+c_{t_2} & 0 & 0 & -c_{s_2} & 0 & -c_{s_2}l_2 & 0 & 0\\
0 & 0 & c_{s_3}+c_{t_3} & 0 & -c_{s_3} & 0 & -c_{s_3}L & -c_{s_3}(l_5+l_6) & -c_{s_3}(l_9-l_3)\\
0 & 0 & 0 & c_{s_4}+c_{t_4} & -c_{s_4} & 0 & -c_{s_4}L & -c_{s_4}(l_5+l_6) & -c_{s_4}(l_9+l_4)\\
-c_{s_1} & -c_{s_2} & 0 & 0 & c_{s_1}+c_{s_2}+c_d & -c_d & -c_{s_1}l_1-c_{s_2}l_2 & 0 & 0\\
0 & 0 & -c_{s_3} & -c_{s_4} & c_{s_3}+c_{s_4} & 0 & c_{s_3}L+c_{s_4}L & (c_{s_3}+c_{s_4})(l_5+l_6) & c_{s_3}(l_9-l_3)+c_{s_4}(l_9+l_4)\\
0 & 0 & 0 & 0 & -c_d & c_d & c_d l_6 & 0 & 0\\
c_{s_1}l_1 & -c_{s_2}l_2 & 0 & 0 & -c_{s_1}l_6-c_{s_1}l_7+c_{s_2}l_6 & c_d l_6 & c_d l_6^2+c_{s_1}l_7^2+c_{s_2}l_7^2 & 0 & 0\\
0 & 0 & c_{s_3}l_3 & -c_{s_4}l_4 & -c_{s_3}l_7+c_{s_4}L & 0 & -c_{s_3}Ll_7+c_{s_4}Ll_4 & -c_{s_3}(l_5+l_6)l_3+c_{s_4}(l_5+l_6)l_4 & -c_{s_3}(l_9-l_3)l_3+c_{s_4}(l_9+l_4)l_4
\end{bmatrix}$$

$$[k]=\begin{bmatrix}
k_{t_1} & 0 & 0 & 0\\
0 & k_{t_2} & 0 & 0\\
0 & 0 & k_{t_3} & 0\\
0 & 0 & 0 & k_{t_4}
\end{bmatrix} \qquad \text{(A-4)}$$

$$[c]=\begin{bmatrix}
c_{t_1} & 0 & 0 & 0\\
0 & c_{t_2} & 0 & 0\\
0 & 0 & c_{t_3} & 0\\
0 & 0 & 0 & c_{t_4}
\end{bmatrix} \qquad \text{(A-5)}$$

Appendix B: Parameter values and units of the truck and full trailer

m_1 = 800 kg
m_2 = 800 kg
m_3 = 800 kg
m_4 = 800 kg
m_5 = 4000 kg
m_6 = 200 kg
m_7 = 3600 kg
m_8 = 100 kg
$I_5 = 8500 kg - m^2$
$I_6 = 45 kg - m^2$
$I_7 = 7500 kg - m^2$
$w_1 = 12400 kg$
$w_2 = 12400 kg$
k_{t_1} = 800000 N/m
k_{t_2} = 800000 N/m
k_{t_3} = 800000 N/m
k_{t_4} = 800000 N/m
k_{s_1} = 80000 N/m
k_{s_2} = 80000 N/m
k_{s_3} = 80000 N/m
k_{s_4} = 80000 N/m

k_d = 4000 N/m
c_{t_1} = 2000 $N-s/m$
c_{t_2} = 2000 $N-s/m$
c_{t_3} = 2000 $N-s/m$
c_{t_4} = 2000 $N-s/m$
c_{s_1} = 30000 $N-s/m$
c_{s_2} = 30000 $N-s/m$
c_{s_3} = 30000 $N-s/m$
c_{s_4} = 30000 $N-s/m$
c_d = 250 $N-s/m$
l_1 = 1.6 m
l_2 = 1.4 m
$l_3 = 1.7m$
l_4 = 1.3 m
l_5 = 0.85 m
l_6 = 0.8 m
l_7 = 2.7 m
l_8 = 2.4 m
l_9 = 1.3 m
l_{10} = 1.0 m
l_{11} = 2.6 m

International Journal of Vehicle Design
HEAVY VEHICLE SYSTEMS
Editor-in-Chief M A Dorgham BSc MSc PhD CEng PEng MIMechE Mem ASME MSAE

Editorial Address: 17 Beeward Close, The Leys,
Wolverton Mill, MILTON KEYNES
Bucks, UK. MK12 6LJ

Tel: National (01908) 314248
International (44 1908) 314248
Fax: International (44 1908) 221509
Email: hvs@inderscience.com

30th December 1998

Dear Professor Wang,

Re: Your paper published in Volume 5 Nos. 3/4 (1998) of Heavy Vehicle Systems (HVS)- A Special Series of the International Journal of Vehicle Design (IJVD).

I enclose a copy of Volume 5 Nos. 3/4 (1998) of *Heavy Vehicle Systems* which includes your published contribution to this important topic. The publication of your paper reflects the high esteem held for you by your fellow professionals.

On behalf of the Editorial Board of the Journal, I would like to thank you for your kind help and support for the Journal and in promoting its objectives. Your help in circulating the enclosed information about the Journal and relevant publications, to libraries and others that might be interested to subscribe to and/or contribute a paper, would be most appreciated.

Best Wishes and Regards.

Yours sincerely,

Dr M A Dorgham
Editor in Chief

Sample Copies of IJSD and IJCEELL are also enclosed.